

## Preparation of LaFeO<sub>3</sub> particles by sol-gel technology

C. Vázquez-Vázquez,<sup>a)</sup> P. Kögerler, and M. A. López-Quintela  
*Department of Physical Chemistry, University of Santiago de Compostela,  
E-15706 Santiago de Compostela, Spain*

R. D. Sánchez and J. Rivas  
*Department of Applied Physics, University of Santiago de Compostela,  
E-15706 Santiago de Compostela, Spain*

(Received 12 February 1996; accepted 21 April 1997)

The study of submicroscopic particles in already known systems has resulted in a renewed interest due to the large differences found in their properties when the particle size is reduced, and because of possible new technological applications. In this work we report the preparation of LaFeO<sub>3</sub> particles by the sol-gel route, starting from a solution of the corresponding metallic nitrates and using urea as gelificant agent. Gels were decomposed at 200 °C and calcined 3 h at several temperatures,  $T$ , in the range 250–1000 °C. The samples were structurally characterized by x-ray diffraction (XRD) showing that the orthoferrite crystallizes at  $T$  as low as 315 °C. From the x-ray diffraction peak broadening, the particle size was determined. The size increases from 60 to 300 nm as the calcination  $T$  increases. Infrared spectroscopy was used to characterize gels and calcined samples. From these studies a mechanism for the gel formation is proposed. Study of the magnetic properties of LaFeO<sub>3</sub> particles shows the presence of a ferromagnetic component which diminishes as the calcination temperature increases, vanishing at  $T = 1000$  °C.

### I. INTRODUCTION

Perovskite-type oxides containing transition metals have been known to show high catalytic activity for the complete oxidation of hydrocarbons, and their potentiality of replacing noble metals as combustion catalysts has been examined extensively.<sup>1,2</sup>

LaFeO<sub>3</sub> is an orthoferrite which crystallizes in the space group  $D_{2h}^{16}$ - $Pbnm$ <sup>3,4</sup> and shows antiferromagnetic order below  $T_N = 740$  K.<sup>5</sup> This material is an orthorhombic distorted version of AMO<sub>3</sub> cubic perovskites (A = Sr, Ca, or a rare earth; M = transition metal; e.g., SrFeO<sub>3</sub>) as a result of steric adjustments when smaller rare-earth elements are substituted at the A sites. The Fe atoms have an oxygen octahedral local environment and the distortion is manifested as a tilting of the octahedra off the  $c$ -axis direction. The degree of tilting is dependent on the size of the A atom and this determines the deviation of the Fe–O–Fe superexchange angle from 180°.<sup>6</sup>

Until now, almost all the studies about these compounds have been performed on single crystals and powders obtained by solid state reaction.<sup>7</sup> This technique, which uses metal oxides as starting materials and needs several annealings at high temperatures during long periods of time with frequent intermediary grindings, has several problems, e.g., poor homogeneity

and high porosity of the samples, no control on the particle size, etc. To avoid these problems, which are common to the synthesis of other type of perovskites, several sol-gel techniques have been developed, showing different advantages compared with the conventional ceramic fabrication techniques. For example, with sol-gel techniques<sup>8–11</sup> high purity and good homogeneity materials require lower processing temperatures and shorter annealing times than conventional techniques, they present a high reproductivity, and they have a good control of the stoichiometry, size, and shape of the particles obtained.

The study of fine and ultrafine particles has gained increasing interest due to the new properties the materials may show when grain size is reduced and, therefore, the new applications that can appear.

In the present work we describe the synthesis of LaFeO<sub>3</sub> microparticles via sol-gel technology, which allows the preparation of polycrystalline powders at lower temperatures than those used by solid state reaction. Samples calcined at several temperatures were prepared in order to study the effect of the calcination temperature on their structural and magnetic properties. Infrared studies were carried out on the gel and its decomposition products, and a mechanism is proposed for the gel formation.

### II. EXPERIMENTAL PROCEDURE

In the synthesis procedures carried out in this work all the reagent-grade chemicals employed were Aldrich

<sup>a)</sup>E-mail address: qfmatcvv@usemail.usc.es

(Steinheim, Germany) and were used without further purification. La<sub>2</sub>O<sub>3</sub>, La(NO<sub>3</sub>)<sub>3</sub> · 6H<sub>2</sub>O and Fe(NO<sub>3</sub>)<sub>3</sub> · 9H<sub>2</sub>O were dried in a vacuum desiccator and stored in an inert glove box before use, because they are highly hygroscopic. In order to obtain a polycrystalline reference pattern, LaFeO<sub>3</sub> was synthesized by solid state reaction. For this purpose, La<sub>2</sub>O<sub>3</sub> and  $\alpha$ -Fe<sub>2</sub>O<sub>3</sub> (hematite) were used as starting materials. A stoichiometric mixture of these reagents was ground in an agate ball mill for 6 h and then annealed 184 h at 1000 °C in several steps with intermediary grindings.

For the synthesis of LaFeO<sub>3</sub> via sol-gel technology using urea as gelificant agent stoichiometric amounts of lanthanum and iron nitrates were used as starting materials, due to their high solubility in water. The initial concentrations were 0.2 M in La(III), 0.2 M in Fe(III), and the urea concentration was fixed at  $\psi = 10$ , with  $\psi = [\text{urea}]/[\text{La(III)}] + [\text{Fe(III)}]$ . The reasons for using this value of  $\psi$  are given elsewhere.<sup>11</sup> The solvent was evaporated directly on a hot plate with continuous stirring at temperatures ranging between 75 and 125 °C. When cooling down, a gel appeared, which was decomposed in an oven at 200 °C in air, yielding a precursor of these samples. After 1 h dry-grinding, the precursor was calcined at several temperatures (ranging between 250 and 1000 °C) in order to study the effect of the calcination temperature on their structural and magnetic properties. Decomposition and calcination were carried out in a Quasar HEM-L-1 furnace in a static air atmosphere with a heating rate of  $\approx 10^\circ\text{C}/\text{min}$ . All the samples were quenched in air to room temperature after calcination.

The structural characterization of the polycrystalline powders was carried out by x-ray powder diffraction, using a diffractometer Philips PW-1710 with Cu anode (radiation Cu K $_{\alpha}$  of  $\lambda = 1.54186 \text{ \AA}$ ). The measurements were performed in air at room temperature. Infrared spectroscopy measurements of the gel were carried out in a Bruker IFS 66V spectrophotometer and calcined samples were measured in a Mattson Cygnus 100 infrared spectrophotometer flushed with dry air. KBr pellets between rock salt plates were used and IR spectra were scanned between 4000 and 400 cm<sup>-1</sup> with a scan resolution of 2 cm<sup>-1</sup> for the Bruker and of 4 cm<sup>-1</sup> for the Mattson spectrophotometers. Magnetization of the samples was measured with a DMS 1660 vibrating sample magnetometer (VSM).

### III. RESULTS AND DISCUSSION

#### A. Infrared spectroscopy: Properties of the gel

The IR spectra of the gel and its calcination products are shown in Fig. 1 and compared with the IR spectrum of urea. In Table I is shown the absorption maxima for urea and their assignments according to Penland

*et al.*<sup>12</sup> The precursor and the products calcined below 315 °C give somewhat complicated spectra, due to the simultaneous presence of urea and its decomposition products, although the bands at 1380 and 830 cm<sup>-1</sup> may be assigned to the nitrate group. We have observed that when the orthoferrite crystallizes, at 315 °C, almost all the organic stuff was removed and only the bands from the nitrate group remained up to 500 °C. The band at 565 cm<sup>-1</sup> may be assigned to the Fe–O stretching.<sup>13</sup>

Hydrogen bonding was observed for the gel and the precursor, surely due to the hydroxide ions, because of the shift of the C=O stretching to lower frequencies (1662 cm<sup>-1</sup>) and the NH<sub>2</sub> bending to higher frequencies (1625 cm<sup>-1</sup>).<sup>14</sup> For the samples calcined at temperatures lower than the orthoferrite crystallization, the presence of a carbonyl vibration at 1725 cm<sup>-1</sup> is also observed, which intensity decreases as the calcination temperature increases. This band indicates that a coordination bond is formed between the nitrogen and the central metal atom.<sup>12</sup> This N → M bond increases the electron demand by the donor nitrogen atom and blocks the resonance between this nitrogen atom and the carbonyl group, increasing the C=O double bond character. For the precursor, we have observed the presence of two bands at lower frequencies (around 3030 cm<sup>-1</sup>) than that from N–H stretching vibrations (3450 and 3350 cm<sup>-1</sup>), which may be assigned to the N–H stretching vibrations of the coordinated NH<sub>2</sub> group.<sup>12</sup> Since free and coordinated N–H frequencies were observed in the spectra, it can be concluded that only one nitrogen atom of each urea molecule coordinates to the central metal ion. Nevertheless, the percentage of N → M bonding decreases as the calcination temperature increases, as can be observed in Fig. 1(b). The formation of the N → M bond implies a more single character for the C–N bond, shifting it to lower frequencies (1450 cm<sup>-1</sup>). For the precursor the bands observed at 1588 and 1633 cm<sup>-1</sup> may be assigned to the free and coordinated NH<sub>2</sub> bonding vibrations. Taking into account all the assignments we can assume the gel network is made by a random distribution of metallic ions crosslinked through hydroxides, nitrates, and urea (O- and N-coordination).

#### B. Mechanism of the gel formation

The role of the urea in the synthesis reaction is very important.<sup>11</sup> In an aqueous solution, metallic ions are coordinated by water molecules, but when an aqueous solution of urea is heated at temperatures  $\geq 75 \text{ }^\circ\text{C}$ , decomposition of urea to CO<sub>3</sub><sup>2-</sup> and NH<sub>3</sub> (with releasing of hydroxide ions) becomes faster.<sup>15</sup> In the absence of acids the following reaction takes place:



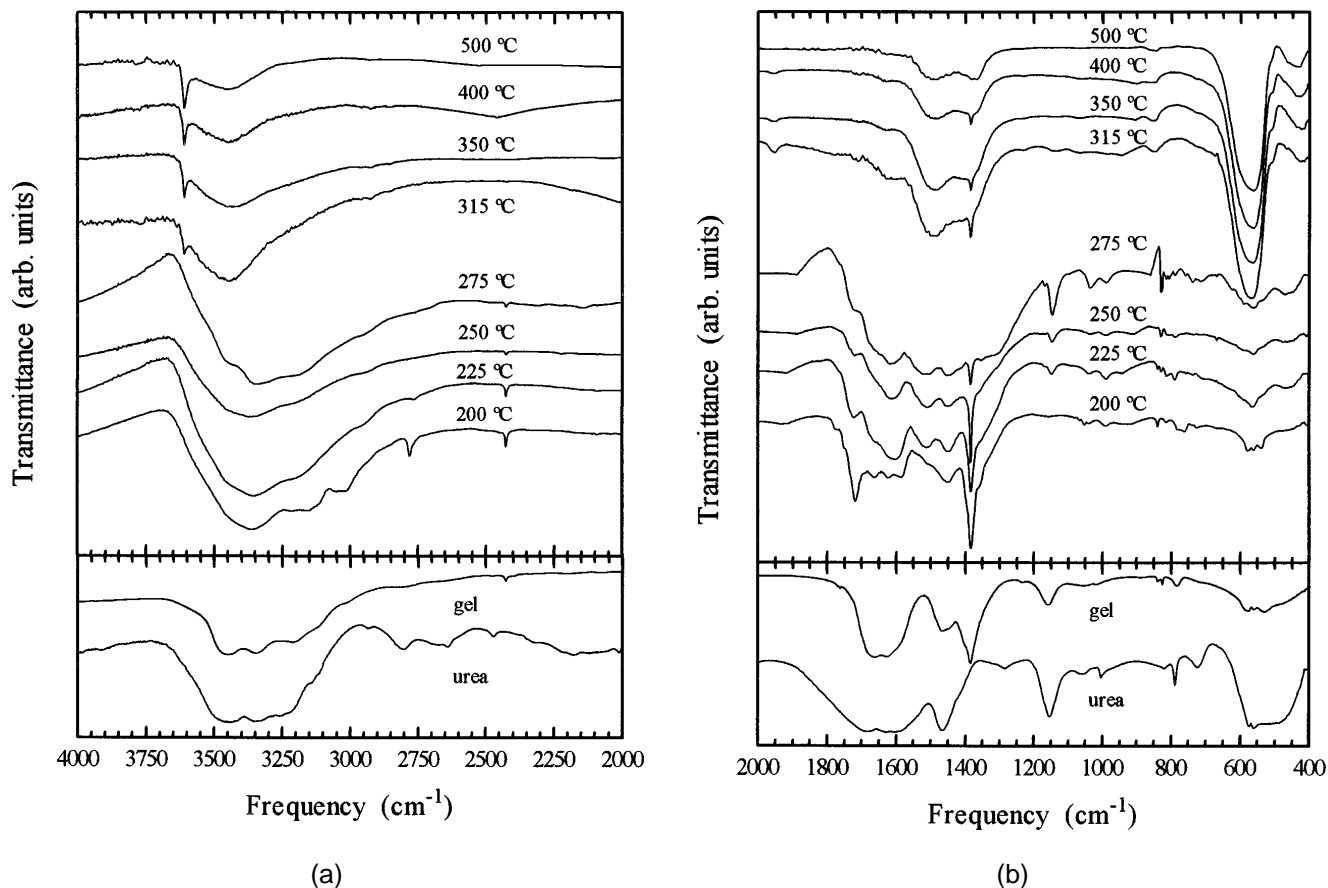


FIG. 1. (a) Infrared spectra evolution as a function of the calcination temperature, 4000–2000 cm<sup>-1</sup>. Lower part shows the IR spectra of the urea and the as-prepared gel. (b) Infrared spectra evolution as a function of the calcination temperature, 2000–400 cm<sup>-1</sup>. Lower part shows the IR spectra of the urea and the as-prepared gel.

TABLE I. Main absorption maxima for urea and their assignments according to Penland *et al.*<sup>12</sup>

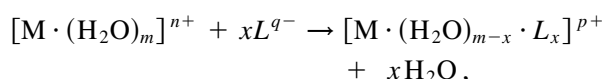
Observed frequencies (cm <sup>-1</sup> )	Type of vibration
3457, 3349, 3260	N–H stretching
1682, 1607	C=O stretching and NH <sub>2</sub> bending
1467	C–N stretching
1154	NH <sub>2</sub> rocking
1004	C–N stretching
573, 559	N–C–O deformation
500	N–C–N deformation

In acid media a rapid quantitative conversion of the cyanate ion to ammonium ion occurs<sup>16</sup>:



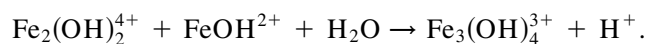
The rate of decomposition depends on the temperature and urea concentration.<sup>16</sup> Some new ligands which can substitute water molecules in their coordination positions around the metal ions (NH<sub>4</sub><sup>+</sup>, OH<sup>-</sup>, CO<sub>3</sub><sup>2-</sup>) appear in solution. The substitution degree of water by other ligands depends on the nature and concentration of metallic ions and ligands. The elimination of water by

evaporation promotes the substitution of water ligands, according to the following scheme:



where M = La(III), Fe(III) and L = NH<sub>3</sub>, OH<sup>-</sup>, CO<sub>3</sub><sup>2-</sup> urea. Urea ligands can coordinate metallic ions through the carbonyl group or the amino group,<sup>12</sup> but Fe(III) coordination occurs through the oxygen of urea.<sup>17</sup> The infrared spectra of tetramethylurea (tmu) complexes of lanthanide elements, [Ln(tmu)<sub>6</sub>](ClO<sub>4</sub>)<sub>3</sub>, indicate the presence of this O-coordination.<sup>18</sup> In our case, infrared spectra have indicated that O-coordination is present in the gel, but in the samples decomposed at temperatures below the LaFeO<sub>3</sub> crystallization some extent of N-coordination was observed.

The initial aqueous solution has an acid pH (≈2.2). This pH remains acid during most of the evaporation process, lowering a little bit as far as water removing goes on due to the formation of polynuclear species,<sup>19</sup> e.g.,



When urea begins to decompose small amounts of precipitate appears. The x-ray pattern of the precipitate indicates that ferrihydrite, Fe<sub>5</sub>O<sub>7</sub>(OH) · 4H<sub>2</sub>O, and La(NO<sub>3</sub>)(OH)<sub>2</sub> · H<sub>2</sub>O are formed, due to the hydroxide ions released during this step. The acid hydrolysis of Fe(III) ions leads to ferrihydrite, as has been proposed by Cornell *et al.*<sup>19</sup> When enough water is evaporated temperature raises decomposing urea faster, increasing the pH due to the ammonia release. When the temperature is around 125 °C (close to the melting point of urea)<sup>20</sup> the mixture is taken out from heating. While the mixture cools down, a gel is formed, due to the condensation of monomers through the hydroxide ligands, forming long chains.<sup>21</sup> Metallic ions will then be located in the gel network with a statistical distribution according to the stoichiometric amounts of these ions in the starting solution. It is to be noted that a small amount of these ions are not statistically distributed in the gel due to the precipitation of some of these ions.

### C. X-ray diffraction

X-ray diffraction patterns of the ceramic samples show that 184 h at 1000 °C are necessary to obtain pure and well crystallized LaFeO<sub>3</sub>. For shorter periods of time x-ray patterns still show peaks of La<sub>2</sub>O<sub>3</sub> and α-Fe<sub>2</sub>O<sub>3</sub> that have not reacted. This sample was used as a standard reference for comparing with the sol-gel samples.

For the sol-gel technology samples it is observed that LaFeO<sub>3</sub> crystallizes at temperatures as low as 315 °C. The x-ray diffraction pattern of the gel decomposed at 200 °C shows a lot of diffraction peaks due to decomposition products which made it very difficult to identify unambiguously the phases present in the samples. The sample calcined at 300 °C shows small broad peaks due to α-Fe<sub>2</sub>O<sub>3</sub> and ferrihydrite (Fe<sub>5</sub>O<sub>7</sub>(OH) · 4H<sub>2</sub>O), which transforms into α-Fe<sub>2</sub>O<sub>3</sub> at higher temperatures. After crystallization all the samples show small peaks from two secondary phases: La(OH)<sub>3</sub> and α-Fe<sub>2</sub>O<sub>3</sub>. In Fig. 2 the results obtained as a function of the calcination temperature are shown. La(OH)<sub>3</sub> and α-Fe<sub>2</sub>O<sub>3</sub> are formed by thermal decomposition of La(NO<sub>3</sub>)(OH)<sub>2</sub> · H<sub>2</sub>O and ferrihydrite, Fe<sub>5</sub>O<sub>7</sub>(OH) · 4H<sub>2</sub>O, which appeared in the precipitate formed during the evaporation of the solvent, as stated above.

An average crystallite size,  $D_{hkl}$ , was determined by applying the Debye–Scherrer formula using the full-width-at-half-maximum (FWHM),  $\beta$ , of the x-ray diffraction peak at  $d \approx 2.778 \text{ \AA}$ :

$$D_{hkl} (\text{\AA}) = \frac{k \cdot \lambda}{\beta(\text{size}) \cdot \cos \Theta},$$

where  $k$  is the shape factor which normally ranges between 0.9 and 1.0 (in our case  $k = 0.9$ ),  $\lambda$  is the x-ray wavelength, and  $\Theta$  the Bragg angle.<sup>22</sup>  $\beta(\text{size})$  is the

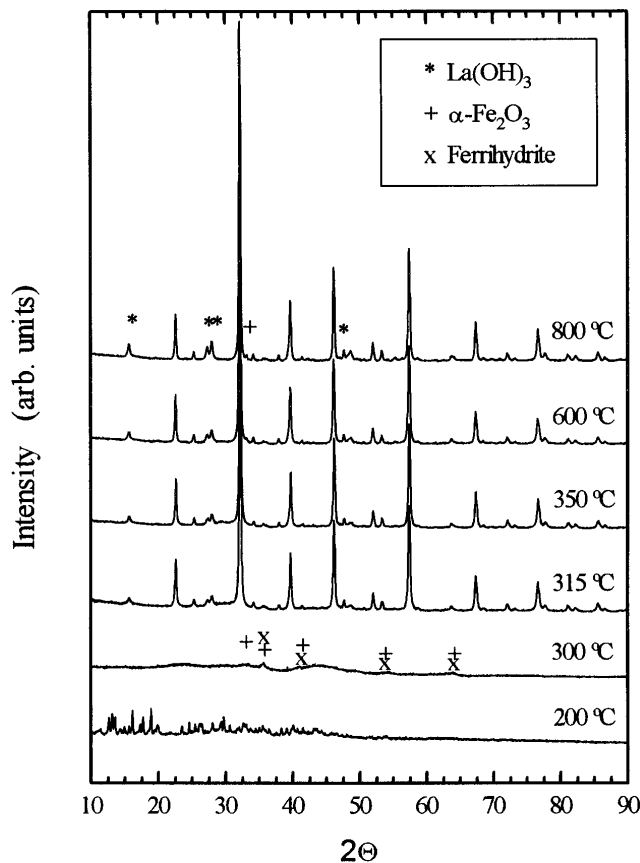


FIG. 2. X-ray diffraction evolution as a function of the calcination temperature.

difference in profile widths of broadened and standard peaks:  $\beta(\text{size}) = \beta_{\text{sample}} - \beta_{\text{standard}}$ . Another physical effect that broadens the profile shape peaks is the lattice microstrain, or mean lattice distortion,  $\epsilon$ . This effect can be taken into account by the following equation:

$$\epsilon = \frac{\beta(\text{strain})}{4 \cdot \tan \Theta},$$

where  $\beta(\text{strain}) = \sqrt{\beta_{\text{sample}}^2 - \beta_{\text{standard}}^2}$ . Results for both crystallite size and microstrain obtained for our samples according to the above equations are shown in Figs. 3(a) and 3(b), respectively, and as expected, a tendency is observed, to an increase on crystallite size and a decrease of the microstrain as the calcination temperature and calcination time increase.

### D. Magnetic properties

Hysteresis loops at room temperature were measured for each calcination temperature. Before LaFeO<sub>3</sub> crystallization the curves show a superparamagnetic (SP) behavior. At 315 °C LaFeO<sub>3</sub> crystallizes and a great change in the magnetic properties takes place, showing a ferromagnetic behavior. When the calcination temperature increases, a decrease in the ferromagnetic order

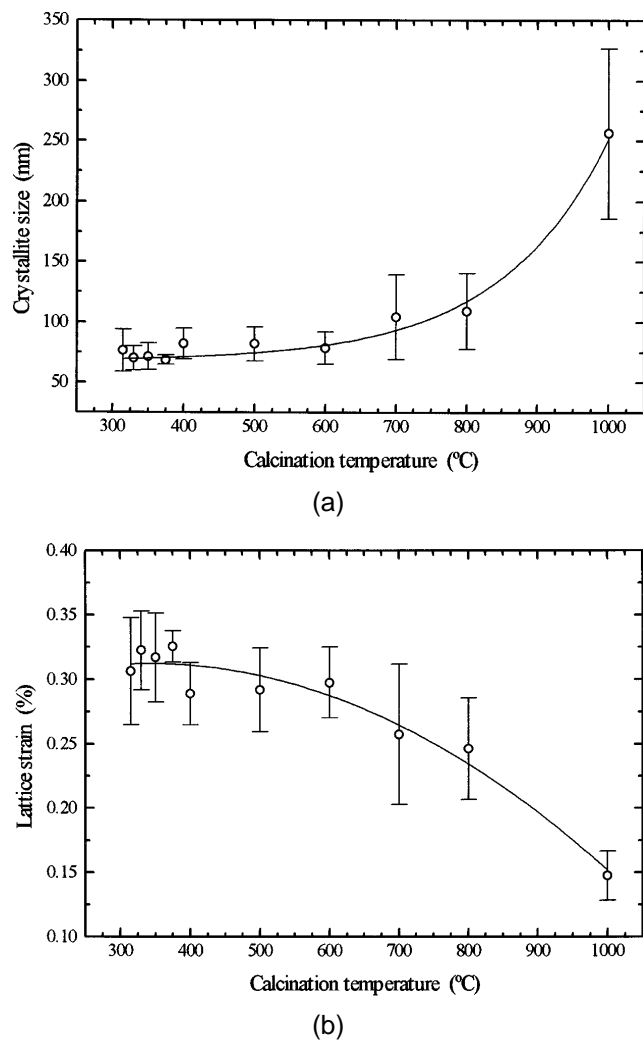


FIG. 3. (a) Crystallite size, determined by using the Debye–Scherrer equation, as a function of the calcination temperature. The continuous line is a guide to eye. (b) Lattice strain, or mean lattice distortion, as a function of the calcination temperature. The continuous line is a guide to eye.

was observed until samples become antiferromagnetic for calcination temperatures near 1000 °C (Fig. 4). In order to understand this behavior, the authors have presented a complete magnetic study in Ref. 23, giving results of Electron Spin Resonance (ESR), Mössbauer spectroscopy, and magnetization versus temperature.

Three magnetic regions were observed with the calcination temperature. At low  $T$ , before the crystallization of LaFeO<sub>3</sub>, the presence of superparamagnetism due to iron oxide particles (mainly,  $\gamma$ -Fe<sub>2</sub>O<sub>3</sub>) was detected. Fitting the hysteresis loops to the Langevin function, an average particle size of 10 nm was determined. At 315 °C, the crystallization of LaFeO<sub>3</sub> induces the organization of the iron oxide changing the magnetic behavior observed at lower temperatures. Between 315 and 700 °C, the amount of iron oxide decreases, with its

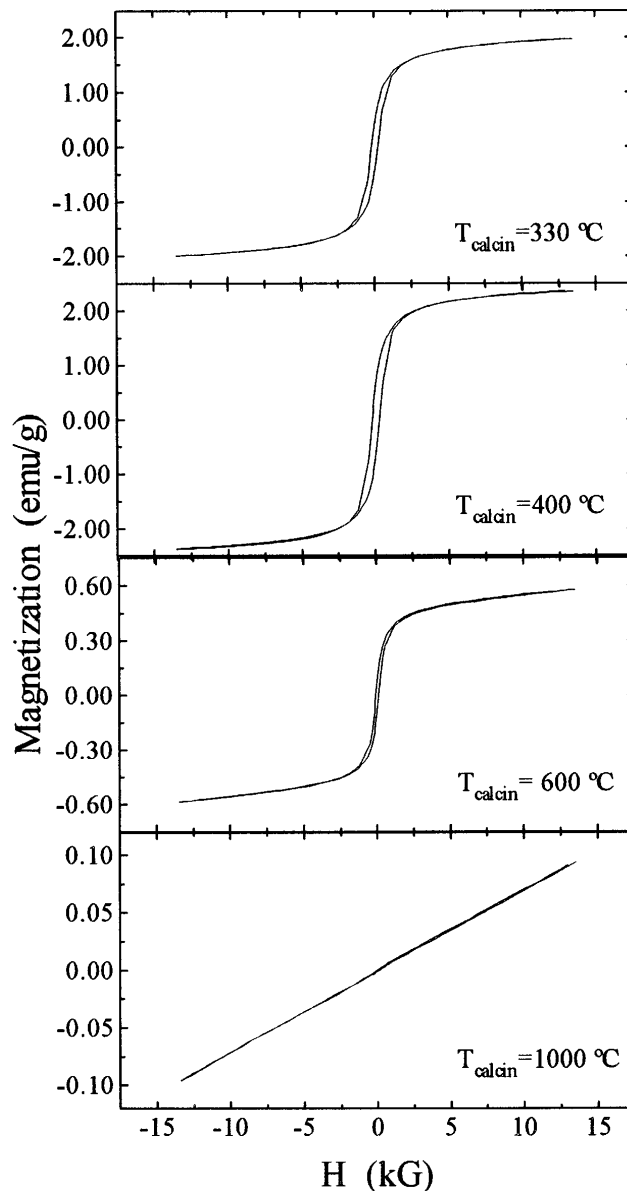


FIG. 4. Hysteresis loops measured at 298 K of LaFeO<sub>3</sub> synthesized at several calcination temperatures.

associated ferromagnetism. The system evolves from a nanocomposite (iron oxide + LaFeO<sub>3</sub>) to a single phase (LaFeO<sub>3</sub>). Above 700 °C the third magnetic region is present, showing similar properties as bulk LaFeO<sub>3</sub>.

#### IV. CONCLUSIONS

We have prepared LaFeO<sub>3</sub> microparticles by sol-gel technology using urea as gelificant agent. We were able to prepare LaFeO<sub>3</sub> at temperatures as low as 315 °C. As the calcination temperature increases, crystallite sizes rise from 60 to 300 nm and lattice microstrains get lower. IR spectra indicate that O-coordination is present

in the gel, but in the samples decomposed at temperatures below LaFeO<sub>3</sub> crystallization, some extent of N-coordination was observed. As far as we know, N-coordination from urea was not reported for Fe(III) and La(III) ions, which usually coordinate through the carbonate group only.<sup>17,18</sup> For the crystallized samples we have observed the presence of a ferromagnetic component which diminishes as the calcination temperature increases, disappearing at high calcination temperatures.

## ACKNOWLEDGMENTS

The authors wish to acknowledge financial support from DGICYT, PB92-1086, and NATO, CRG920255. C. V.-V. also thanks Xunta de Galicia for its financial support.

## REFERENCES

1. G. Karlsson, *Electrochim. Acta* **30** (11), 1555–1561 (1985).
2. A. Hammouche, E. Siebert, and A. Hammou, *Mater. Res. Bull.* **24**, 267–280 (1989).
3. H. McMurdie, M. Morris, E. Evans, B. Paretzkin, W. Wong-Ng, and C. Hubbard, *Powd. Diff.* **1**, 269 (1986).
4. M. Marezio and P. D. Dernier, *Mater. Res. Bull.* **6**, 23–30 (1971).
5. R. D. Sánchez, R. E. Carbonio, and M. T. Causa, *J. Magn. Magn. Mater.* **140–144**, 2147–2148 (1995).
6. M. Eibschutz, S. Shtrikman, and D. Treves, *Phys. Rev.* **156**, 562 (1967).
7. M. F. Yan, H. C. Ling, H. M. O'Bryan, P. K. Gallagher, and W. W. Rhodes, *IEEE Trans. Components, Hybrids, Manuf. Technol.* **11** (4), 401 (1988).
8. G. Kordas, *J. Non-Cryst. Solids* **121**, 436–442 (1990).
9. P. F. James, in *The 2nd European Conference on Advanced Materials and Processes, EUROMAT'91*, 350–351, University of Cambridge, U.K. (1991).
10. S. Sakka, *Mater. Res. Soc.* 221–232 (1989).
11. J. Mahía, C. Vázquez-Vázquez, M. I. Basadre-Pampín, J. Mira, J. Rivas, M. A. López-Quintela, and S. B. Oseroff, *J. Am. Ceram. Soc.* **79** (2), 407–411 (1996).
12. R. B. Penland, S. Mizushima, C. Curran, and J. V. Quagliano, *J. Am. Chem. Soc.* **79**, 1575 (1957).
13. G. V. Subba Rao, C. N. R. Rao, and J. R. Ferraro, *Appl. Spectrosc.* **24** (4), 436–445 (1970).
14. R. T. Conley, in *Infrared Spectroscopy*, 2nd ed. (Allyn and Bacon, Inc., Boston, MA, 1972), pp. 167–168.
15. E. Matijević and W. P. Hsu, *J. Colloid Interface Sci.* **118**, 506–523 (1987).
16. W. H. R. Shaw and J. J. Bordeaux, *J. Am. Chem. Soc.* **77**, 4729–4733 (1955).
17. A. Yamaguchi, T. Miyazawa, T. Shimanouchi, and S. Mizushima, *Spectrochim. Acta* **10**, 170 (1957).
18. E. Giesbrecht and M. Kawashita, *J. Inorg. Nucl. Chem.* **32**, 2461 (1970).
19. R. M. Cornell, R. Giovanoli, and W. Schneider, *J. Chem. Technol. Biotechnol.* **46**, 115–134 (1989).
20. F. W. Miller, Jr. and H. R. Dittmar, *J. Am. Chem. Soc.* **56**, 848–849 (1934).
21. J. Livage, M. Henry, and C. Sánchez, *Progr. Solid State Chem.* **18**, 259–341 (1988).
22. International Union of Crystallography, *International Tables for X-ray Crystallography*, part III, 318–323, Dordrecht, The Netherlands (1985).
23. R. D. Sánchez, J. Rivas, C. Vázquez-Vázquez, M. A. López-Quintela, and J. M. Greneche, unpublished.